Floquet Hopf Insulators

Thomas Schuster, Snir Gazit, Joel E. Moore, and Norman Y. Yao

Phys. Rev. Lett. **123**, 266803 — Published 30 December 2019

DOI: 10.1103/PhysRevLett.123.266803

Floquet Hopf Insulators

Thomas Schuster,[1] Snir Gazit,[2,1] Joel E. Moore,[1,3] and Norman Y. Yao[1,3]

[1] *Department of Physics, University of California, Berkeley, California 94720 USA*
[2] *Racah Institute of Physics and the Fritz Haber Center for Molecular Dynamics, The Hebrew University, Jerusalem 91904, Israel*
[3] *Materials Science Division, Lawrence Berkeley National Laboratory, Berkeley, California 94720, USA*

(Dated: October 29, 2019)

We predict the existence of a Floquet topological insulator in three-dimensional two-band systems, the Floquet Hopf insulator, which possesses two *distinct* topological invariants. One is the Hopf $\mathbb{Z}$ invariant, a linking number characterizing the (non-driven) Hopf topological insulator. The second invariant is an intrinsically Floquet $\mathbb{Z}_2$ invariant, and represents a condensed matter realization of the topology underlying the Witten anomaly in particle physics. Both invariants arise from topological defects in the system's time-evolution, subject to a process in which defects at different quasienergy exchange even amounts of topological charge. Their contrasting classifications lead to a measurable physical consequence, namely, an unusual bulk-boundary correspondence where gapless edge modes are topologically protected, but may exist at *either* 0- or π-quasienergy. Our results represent a phase of matter beyond the conventional classification of Floquet topological insulators.

Periodically driven systems host a rich variety of phases of matter, many of which cannot be realized by any static Hamiltonian [1–9]. Prime representatives of this are the so-called Floquet topological insulators (FTIs): non-interacting, driven phases of matter, whose physical properties are characterized by a set of underlying quantized topological invariants [10–19]. Unlike their non-driven counterparts, the topology of FTIs arises directly from the unitary time-evolution, leading to robustly protected gapless edge modes even when the stroboscopic time-evolution is topologically trivial.

A common pattern has emerged in the classification of Floquet topological insulators, which relates their topological invariants to those of static topological insulators with the same dimension and symmetries. A given FTI is found to possess all the invariants of its static counterpart, plus one additional invariant of *identical* classification. Intuitively, this is understood by extending the bulk-boundary correspondence to Floquet systems: under periodic modulation, the energy – now, quasienergy – becomes defined only modulo 2π (in units of the driving frequency) and thus an additional and identically classified edge mode emerges, associated with the bulk gap at quasienergy π.

This result has been established rigorously in systems described by K-theory [19], and explored at great length in the context of specific symmetries and dimensionality [10, 13, 15–18]. Nevertheless, one could wonder whether these arguments leave room for more unique topology in Floquet phases that escape this stringent bulk-boundary correspondence.

In this Letter we answer the above inquiry in the affirmative, demonstrating a three-dimensional Floquet topological insulator characterized by two *distinct* topological invariants: a 'static' $\mathbb{Z}$ invariant, and a uniquely Floquet $\mathbb{Z}_2$ invariant. At the heart of our proposal is the Hopf insulator (HI) [20–27], a 3D topological insulator (TI) in the absence of symmetries, which exists beyond the standard K-theoretic classification [28, 29] via its restriction to two-band systems. The $\mathbb{Z}$ invariant of our system is precisely the Hopf invariant of this insulator. The $\mathbb{Z}_2$ invariant replaces the expected additional integer invariant, and characterizes the same topology that underlies the Witten anomaly in (3+1)D $SU(2)$ gauge theories [30–34]. In our context, it can be understood both as a twisting number extension of the Hopf invariant, as well as in terms of gapless topological defects of the Floquet evolution. These 'Hopf' defects may smoothly exchange even amounts of their topological charge, which leads to the reduced $\mathbb{Z}_2$ classification. Physically, the difference in invariants creates an atypical bulk-boundary correspondence, where gapless edge modes are topologically pro-

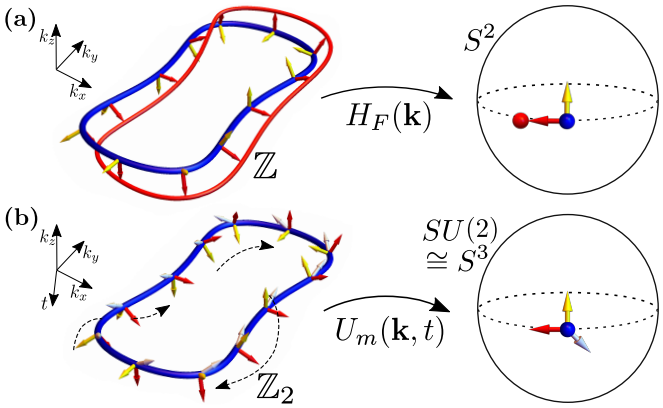

FIG. 1. Depiction of the Floquet Hopf insulator's two topological invariants. **(a)** The 'static' $\mathbb{Z}$ invariant is the Hopf invariant of the Floquet Hamiltonian $H_F(\mathbf{k})$, corresponding to the linking number of the pre-images of two points (blue, red) on the Bloch sphere. For nearby points, this equals the twisting of the Jacobian (colored arrows) along a single pre-image. **(b)** The 'Floquet' $\mathbb{Z}_2$ invariant classifies the micromotion operator $U_m(\mathbf{k},t) \in SU(2)$, and is similarly interpreted as the Jacobian twisting (dashed black arrows) along a pre-image, with a reduced classification due to the larger dimensionality.

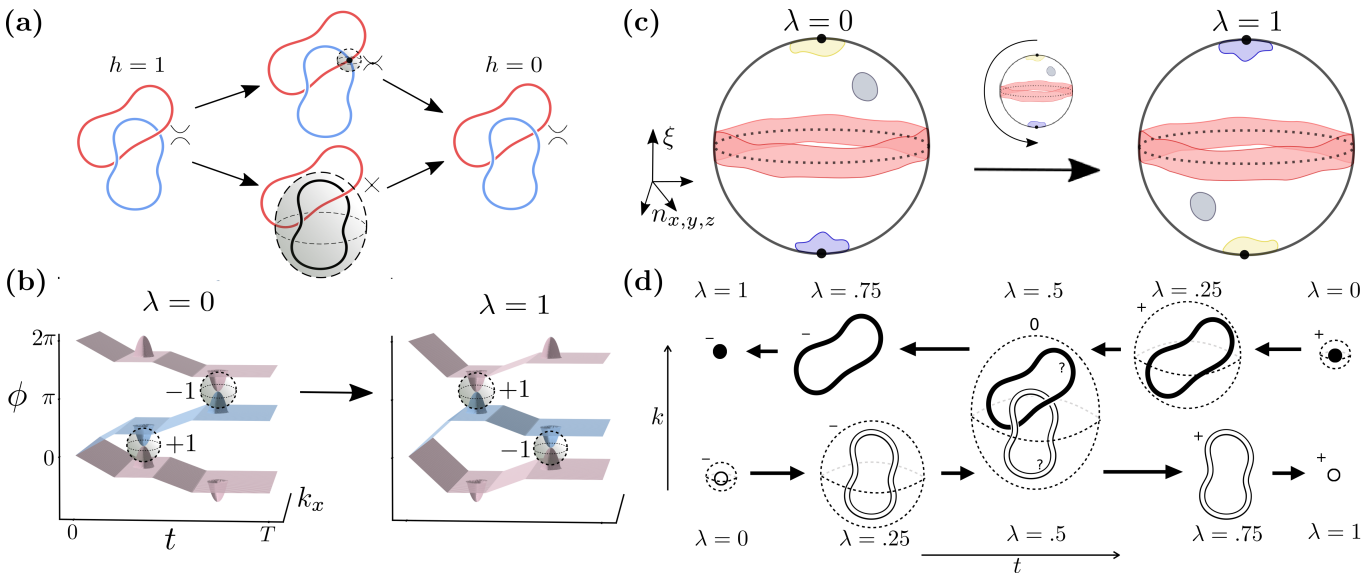

FIG. 2. **(a)** A point Hopf defect (black point) has quadratic dispersion, functioning as a strand crossing that changes the linking number of any two eigenvectors' pre-images (red and blue). A loop Hopf defect (black loop) has linear dispersion, and can occur along a former pre-image. The defect charge is defined on a surface (gray, shaded) enclosing the defect. **(b)** Two Floquet evolutions with different defect charges but the same topological invariants, which are connected by a smooth deformation $\lambda \in [0,1]$ preserving the Floquet unitary's band gaps. **(c)** The deformation is a π rotation of the 3-sphere parameterized by $(\mathbf{n},\xi)$. Images of time-slices representing the initial 0-defect (yellow), π-defect (blue), trivial Hopf invariant (gray), Hopf invariant 1 (red), are displayed before and after the rotation. **(d)** During the deformation, the 0-defects (black outline) and π-defects (solid black) become loops that *link* in the Brillouin zone, at which point their individual charges are undefined. The total charge $h_0 + h_\pi$ is conserved, corresponding to the static $\mathbb{Z}$ invariant. Arrows indicate increasing λ.

tected but may occur at either 0- or π-quasienergy, depending on non-universal properties of the boundary.

We are concerned with non-interacting systems governed by a space- and time-periodic Hamiltonian, written in momentum-space as $H(\mathbf{k},t) = H(\mathbf{k},t+T)$, where $H(\mathbf{k},t)$ is a matrix acting on the internal degrees of freedom that form the two bands of the system. Time-evolution is captured by the unitary operator $U(\mathbf{k},t) = \mathcal{T}\left(e^{-i\int_0^t H(\mathbf{k},t')dt'}\right)$, $0 \le t < T$. Much like static insulators, one can view these unitaries in terms of the band-structures composed by their eigenvectors and eigenphases. For a two-band unitary we write

$$U(\mathbf{k},t) = e^{i\phi}\,|z\rangle\langle z| + e^{i\phi'}\,|z'\rangle\langle z'|\,, \tag{1}$$

where $\phi^{(\prime)}(\mathbf{k},t)$, $\left|z^{(\prime)}(\mathbf{k},t)\right\rangle$ depend on time as well as momentum, and the quasienergies $\phi^{(\prime)}(\mathbf{k},t)$ are periodic.

Floquet topological insulators are Floquet-Bloch systems where the unitary is gapped *at time* T. The Floquet unitary, $U(\mathbf{k},T)$, is equivalently described by the fictitious, time-independent Floquet Hamiltonian, $H_F(\mathbf{k}) = -i\log(U(\mathbf{k},T))/T$. Similar to static TIs, two FTIs are in the same phase if one can smoothly interpolate between them without closing the gaps of the Floquet unitary. Focusing on systems with two gaps for simplicity, recent work has shown that – in all settings with non-driven analogues (i.e. in the absence of explicitly Floquet symmetries, e.g. time-glide symmetry [35]) – such FTIs are characterized by *two* topological invariants, each with the same classification as a static TI of the same dimension and symmetries [10, 13, 15–19, 35].

Here, we note a finer distinction in the classification of FTIs with fixed band number. We decompose the unitary evolution into two components: the evolution over a full period, captured by the Floquet unitary $U(\mathbf{k},T)$, and that within a period, captured by the micromotion unitary, $U_m(\mathbf{k},t) \equiv U(\mathbf{k},t)\left[U(\mathbf{k},T)\right]^{-t/T}$. From this decomposition, one sees that the classification factorizes into two, potentially distinct, invariants: a 'static' invariant classifying the Floquet Hamiltonian $H_F(\mathbf{k})$, and an intrisically Floquet invariant classifying the micromotion operator $U_m(\mathbf{k},t)$. In d space dimensions, the former classifies maps from the dD Brillouin zone to the set of gapped Hamiltonians, identical to the scheme for static TIs. The Floquet invariant classifies maps from the $(d{+}1)$D Floquet Brillouin zone, parameterized by $(\mathbf{k},t)$, to $SU(n)$, for an n-band system without symmetries [13]. These invariants are identical in all cases previously considered. However, for systems with fixed band number they may differ.

We now introduce the Floquet Hopf insulator, a three-dimensional Floquet-Bloch system with two bands and no symmetries. The static invariant is the Hopf invariant of the Floquet Hamiltonian, which we briefly review. The gapped two-band Hamiltonian $H_F(\mathbf{k}) = \mathbf{n}(\mathbf{k})\cdot\boldsymbol{\sigma}$ maps

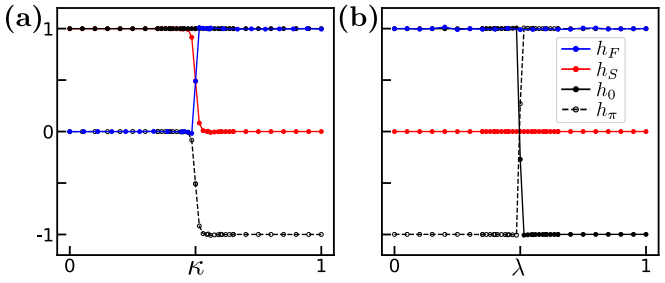

FIG. 3. Numerical calculation of the Floquet invariant, static invariant, and $0/\pi$-defect charges **(a)** across a phase transition $(h_S, h_F) = (1,0) \to (0,1)$ $(\kappa = 0 \to 1)$ **(b)** along the smooth deformation exchanging defect charge.

the 3D Brillouin zone to the Bloch sphere S^2. Neglecting "weak" lower-dimensional invariants [20, 36], such maps are classified by the homotopy group $\pi_3(S^2) = \mathbb{Z}$, thus possessing an integer topological invariant – the Hopf invariant. Expressed in terms of the eigenvectors $|z(\mathbf{k},T)\rangle$ of the Floquet unitary, it takes the form $h_S = \frac{1}{2}\int d^3\mathbf{k}\,\epsilon^{ijk}\,\mathcal{A}_i\,\mathcal{F}_{jk}$, defining the Berry connection $\mathcal{A}_i = \frac{-i}{4\pi}(\langle z|\partial_i z\rangle - \langle \partial_i z|z\rangle)$ and curvature $\mathcal{F}_{jk} = \frac{-i}{4\pi}(\langle \partial_j z|\partial_k z\rangle - \langle \partial_k z|\partial_j z\rangle)$, and where $|z(\mathbf{k},T)\rangle$ is related to the Bloch sphere $\mathbf{n}(\mathbf{k})$ by $\mathbf{n}(\mathbf{k}) = \langle z(\mathbf{k},T)|\,\boldsymbol{\sigma}\,|z(\mathbf{k},T)\rangle$.

The Hopf invariant has an intriguing visual interpretation as a linking number. To elaborate, consider the pre-image of any $\mathbf{n}'$ on the Bloch sphere, i.e. the set of all $\mathbf{k}$ that are mapped to $\mathbf{n}'$ by $\mathbf{n}(\mathbf{k})$. This is generically a 1D loop in the Brillouin zone. The topology of the HI enters when one considers two such pre-images. In the HI phase, any two pre-images are *linked*, with a linking number equal to the Hopf invariant. Intriguingly, this linking can be equivalently viewed as a *twisting* of the Jacobian of $\mathbf{n}(\mathbf{k})$ along a single pre-image [24, 37] (Fig. 1).

We now turn to the Floquet invariant. The micromotion operator maps the 4D Floquet Brillouin zone to $SU(2)$, isomorphic to the 3-sphere S^3. Again neglecting weak invariants, this is classified by the group $\pi_4(S^3) = \mathbb{Z}_2$: a parity invariant, different from the integer Hopf invariant! This invariant was previously studied as the foundation of the Witten anomaly in $SU(2)$ gauge theories, where a formula for it was introduced [31]. In terms of the micromotion operator's eigenvectors $|z_m(\mathbf{k},t)\rangle$ and their relative eigenphase $\Delta\phi_m(\mathbf{k},t)$, we find [38]

$$h_F = \frac{1}{4\pi}\int dt\, d^3\mathbf{k}\,\epsilon^{ijkl}\,\partial_i\Delta\phi_m(\mathbf{k},t)\,\mathcal{A}_j\,\mathcal{F}_{kl} \mod 2, \quad (2)$$

where the Berry connection and curvature are defined analogous to the non-driven case, now over space-time indices $\{k_x, k_y, k_z, t\}$. The Floquet invariant also relates to the Jacobian twisting along a 1D pre-image, now in (3+1)D (Fig. 1). The higher dimensionality leads to the reduced $\mathbb{Z}_2$ classification [37, 38].

Combining the two invariants, we conclude that the Floquet Hopf insulator has a $\mathbb{Z}\times\mathbb{Z}_2$ classification. A system with arbitrary (h_S, h_F) can be generated by strobing two flat band Hamiltonians according to

$$H_{(h_S,h_F)}(\mathbf{k},t) = \begin{cases} \frac{2\pi}{T}H_{h_S-h_F}(\mathbf{k}) & 0 \le t < T/2 \\ -\frac{\pi}{T}H_{h_S}(\mathbf{k}) & T/2 \le t < T \end{cases}, \quad (3)$$

where $H_h(\mathbf{k})$ has Hopf invariant h and energies ± 1. To verify the static invariant, note that the Floquet unitary is given by $U(\mathbf{k},T) = -e^{i\frac{\pi}{2}H_{h_S}}$, whose bands correctly have Hopf invariant h_S. The Floquet invariant is also verified [38]: schematically, the contributions of the two halves of the evolution subtract, giving Floquet invariant $h_S - (h_S - h_F) = h_F \mod 2$.

It is illuminating to discuss how the Floquet Hopf insulator fits in the context of Ref. [17]. Here one again views the evolution in terms of bands, with particular attention to fixed time-slices. If the unitary $U(\mathbf{k},t)$ is gapped at time t, one may define an instantaneous *static* topological invariant $\mathcal{C}(t)$ from its bands, exactly as one defines the static invariant of the Floquet unitary at time $t = T$. This invariant must be constant throughout each gapped region of the evolution, and can only change at times containing gapless points. Such points are *topological defects* of the evolution, and possess a defect charge equal to the total change in $\mathcal{C}(t)$ across the defect. They come in two varieties, 0- and π-defects, labelled by the quasienergy at which the gap closes. The total charges of the 0- and π-defects are locally conserved, and are thereby identified as the topological invariants of the evolution. For example, in the Floquet Chern insulator [13] the instantaneous Chern number changes at gapless Weyl points [39], and the integer charges of the 0- and π-Weyl points comprise a $\mathbb{Z}\times\mathbb{Z}$ classification [17].

Like other topological defects, Hopf topological defects possess an integer charge $h_{0/\pi}$ equal to the change in the instantaneous Hopf invariant across the defect. Two types of Hopf defect exist, each depicted in Fig. 2(a). The first occurs a single gapless point with a quadratic energy degeneracy. Interestingly, the Hopf invariant may also change across *loops* of gapless points, with linear degeneracy. The loops feature a Weyl cone [39] at each point, with the frame of the Weyl cone rotating by $2\pi\Delta h$ about the loop [25, 38].

How does conservation of the two integer defect charges reconcile with the correct $\mathbb{Z}\times\mathbb{Z}_2$ classification? The answer lies in a smooth deformation that exchanges even charge between the 0- and π-defects, such that $(h_0, h_\pi) \to (h_0 - 2, h_\pi + 2)$. This process has no analogue in previously studied FTIs and keeps both band gaps of the Floquet unitary open, establishing the two configurations as the same phase. The total charge $h_0 + h_\pi$ is conserved in this process, while the individual charge h_π is only conserved mod 2. This suggests the identifications

$$\begin{aligned} h_S &= h_0 + h_\pi \quad \in \mathbb{Z} \\ h_F &= h_\pi \bmod 2 \in \mathbb{Z}_2. \end{aligned} \quad (4)$$

The former follows from the definition of defect charge: the invariant at $t = T$ equals the sum of all changes to it throughout the evolution. We explicitly describe the above deformation for the specific case of $(h_0, h_\pi) = (1, -1) \to (-1, 1)$, finding a continuous family of evolutions $U(\mathbf{k}, t; \lambda)$ with defect charges $(1, -1)$ at $\lambda = 0$ and $(-1, 1)$ at $\lambda = 1$ [Fig. 2(b)]. Recall that $SU(2)$ is topologically equivalent to the 3-sphere via the parameterization $U(\mathbf{k}, t) = \xi(\mathbf{k}, t)\, \mathbb{1} + i\mathbf{n}(\mathbf{k}, t) \cdot \boldsymbol{\sigma}$, $\xi^2 + \mathbf{n}(\mathbf{k})^2 = 1$. The deformation acts as a time-dependent rotation of $U(\mathbf{k}, t)$ in the ξn_z-plane: $U(\mathbf{k}, t; \lambda) = R_{\xi n_z}[\lambda\theta(t)]\{U(\mathbf{k}, t)\}$, where the rotation angle $\lambda\theta(t)$ interpolates from 0 at $t = 0$ to $\lambda\pi$ at times after the earliest defect.

To observe that this interpolates between the two configurations without closing the Floquet gap, we examine five regions of the $\lambda = 0, 1$ evolutions [Fig. 2(c)]. Throughout the deformation, the early and late gapped regions remain gapped with trivial topology. The middle region at $\lambda = 1$ is gapped with eigenvectors that can be smoothly deformed to $-\mathbf{n}$, which has the *same* Hopf invariant as the eigenvectors $\mathbf{n}$ at $\lambda = 0$ [40]. Critically, this equivalence does *not* hold for TIs described by K-theory (e.g. the Chern insulator). Finally, the deformation interchanges the location of the 0- and π- defects. Since the intermediate invariant is unchanged, the defect charges are flipped by the deformation.

What allows the seemingly-conserved defect charges to change? Recall how defect charge is rigorously defined: one encloses the defect with a surface of gapped points, and computes the static topological invariant of the surface's eigenvectors [17]. As shown in Fig. 2(d), during the deformation the defects become loops of gapless points. At some value of λ, the 0- and π-defect loops *link* such that it is impossible to separately enclose each defect, causing the individual defect charges to be undefined. This defect linking arises directly from the linking of the HI [38]. After linking, the defects again have well-defined charges, which may differ from their initial values.

We compute the invariants and defect charges numerically in two scenarios (Fig. 3). Across a phase transition $(h_S, h_F) = (1, 0) \to (0, 1)$, both the invariants and defect charges change, following Eq. (4). In contrast, along the smooth deformation, the invariants remain robustly quantized while the defects exchange charge [38].

Like its static counterpart [20, 21, 27], the Floquet Hopf insulator features gapless edge modes at smooth boundaries between phases with different topological invariants (Fig. 4) [38]. An unusual situation occurs at boundaries where the static invariant changes, but the defect charge parities do not. Here, a gap closing is protected by the change in invariant, but may occur at either 0- *or* π-quasienergy, depending on details of the edge region. The anomalous $\mathbb{Z} \times \mathbb{Z}_2$ classification is precisely what allows this ambiguity: since the defect charges are only defined up to parity, neither quasienergy individually requires a gap closing, despite the change in topological invariant.

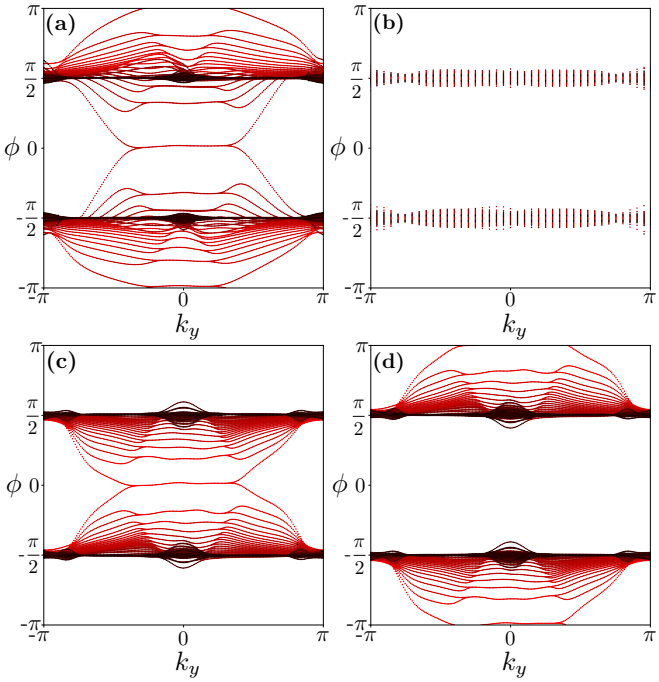

FIG. 4. Quasienergy spectra of the Floquet unitary at various smooth boundaries between Floquet Hopf insulator phases, solved via exact diagonalization [38]. Quasienergies are colored according to their eigenstates' average distance from the edge region, from localized at the edge (red) to far from the edge (black). **(a)** The boundary between $(h_S, h_F) = (0, 1)$ and the trivial phase $(h_S, h_F) = (0, 0)$, features gapless edge modes across both band gaps despite the Floquet Hamiltonian being trivial. **(b)** In contrast, we find no gapless edge modes between phases with different topological defect charges $(h_0, h_\pi) = (1, -1)$ and $(-1, 1)$, but the same topological invariants $(h_S, h_F) = (0, 1 \bmod 2)$, demonstrating the $\mathbb{Z}_2$ classification of the Floquet invariant. **(c,d)** Two different boundaries between the same two phases, $(h_S, h_F) = (2, 0)$ and the trivial phase $(h_S, h_F) = (0, 0)$, featuring gapless edge modes across either the 0- or π-gap.

We now briefly outline potential routes for experimentally realizing the Floquet Hopf insulator. A detailed proposal for realizing the static version of the Hopf insulator in dipolar spin systems was recently introduced in [27]. Interestingly, *any* realization of the static HI provides a direct path to realizing the Floquet Hopf insulator, using the stroboscopic construction of Eq. (3). For example, strobing a Hamiltonian with Hopf invariant 1 with a trivial Hamiltonian realizes the phase $h_S = 0, h_F = 1$. Time-evolving under a trivial Hamiltonian is straightforward: for instance, if the two bands arise from two sublattices, stroboscopic trivial time-evolution can be achieved by modulating the chemical potential on only a single sublattice. As a specific example, in the case of ultracold dipolar molecules [41–44], a staggered chemical potential between two different spatial sublattices can be achieved by using different intensities of light [27]. Fi-

nally, the most interesting, and direct, physical signature of the Floquet Hopf insulator is its complex structure of gapless edge modes, and recent advances in the context of KRb experiments [43, 44] suggest that the presence of such modes can be probed using molecular gas microscopy [27].

Note added: After completing this work, we became aware of Ref. [45], which also finds a $\mathbb{Z}_2$ index characterizing two-band Floquet-Bloch systems in three dimensions and discusses its relation to the Witten anomaly. We note that this index comprises only part of the larger $\mathbb{Z} \times \mathbb{Z}_2$ topological structure we present. Connected to this difference, we note that the edge numerics of Ref. [45] are performed for sharp terminations of the lattice, which in our model are unrepresentative of general edges [38].

[1] R. Moessner and S. Sondhi, Nature Physics **13**, 424 (2017).
[2] J. Zhang, P. Hess, A. Kyprianidis, P. Becker, A. Lee, J. Smith, G. Pagano, I.-D. Potirniche, A. C. Potter, A. Vishwanath, *et al.*, Nature **543**, 217 (2017).
[3] S. Choi, J. Choi, R. Landig, G. Kucsko, H. Zhou, J. Isoya, F. Jelezko, S. Onoda, H. Sumiya, V. Khemani, *et al.*, Nature **543**, 221 (2017).
[4] P. Titum, E. Berg, M. S. Rudner, G. Refael, and N. H. Lindner, Physical Review X **6**, 021013 (2016).
[5] L. J. Maczewsky, J. M. Zeuner, S. Nolte, and A. Szameit, Nature communications **8**, 13756 (2017).
[6] V. Khemani, A. Lazarides, R. Moessner, and S. L. Sondhi, Physical review letters **116**, 250401 (2016).
[7] C. W. von Keyserlingk and S. L. Sondhi, Physical Review B **93**, 245145 (2016).
[8] M. H. Kolodrubetz, F. Nathan, S. Gazit, T. Morimoto, and J. E. Moore, Phys. Rev. Lett. **120**, 150601 (2018).
[9] L. Li, C. H. Lee, and J. Gong, Phys. Rev. Lett. **121**, 036401 (2018).
[10] T. Kitagawa, E. Berg, M. Rudner, and E. Demler, Physical Review B **82**, 235114 (2010).
[11] Z. Gu, H. A. Fertig, D. P. Arovas, and A. Auerbach, Phys. Rev. Lett. **107**, 216601 (2011).
[12] N. H. Lindner, G. Refael, and V. Galitski, Nature Physics **7**, 490 (2011).
[13] M. S. Rudner, N. H. Lindner, E. Berg, and M. Levin, Physical Review X **3**, 031005 (2013).
[14] M. C. Rechtsman, J. M. Zeuner, Y. Plotnik, Y. Lumer, D. Podolsky, F. Dreisow, S. Nolte, M. Segev, and A. Szameit, Nature **496**, 196 (2013).
[15] J. K. Asbóth, B. Tarasinski, and P. Delplace, Physical Review B - Condensed Matter and Materials Physics **90**, 1 (2014), 1405.1709.
[16] D. Carpentier, P. Delplace, M. Fruchart, and K. Gawedzki, Physical review letters **114**, 106806 (2015).
[17] F. Nathan and M. S. Rudner, New Journal of Physics **17**, 125014 (2015).
[18] M. Fruchart, Physical Review B **93**, 115429 (2016).
[19] R. Roy and F. Harper, Physical Review B **96**, 155118 (2017).
[20] J. E. Moore, Y. Ran, and X.-G. Wen, Physical Review Letters **101**, 186805 (2008).
[21] D.-L. Deng, S.-T. Wang, C. Shen, and L.-M. Duan, Physical Review B **88**, 201105 (2013).
[22] D.-L. Deng, S.-T. Wang, and L.-M. Duan, Physical Review B **89**, 075126 (2014).
[23] D.-L. Deng, S.-T. Wang, K. Sun, and L.-M. Duan, Chinese Physics Letters **35**, 013701 (2018).
[24] R. Kennedy, Physical Review B **94**, 1 (2016), 1604.02840.
[25] C. Liu, F. Vafa, and C. Xu, Physical Review B **95**, 161116 (2017).
[26] X.-X. Yuan, L. He, S.-T. Wang, D.-L. Deng, F. Wang, W.-Q. Lian, X. Wang, C.-H. Zhang, H.-L. Zhang, X.-Y. Chang, and L.-M. Duan, Chinese Physics Letters **34**, 060302 (2017).
[27] T. Schuster, F. Flicker, M. Li, S. Kotochigova, J. E. Moore, J. Ye, and N. Y. Yao, arXiv preprint arXiv:1901.08597 (2019).
[28] A. Kitaev, in *AIP Conference Proceedings*, Vol. 1134 (AIP, 2009) pp. 22–30.
[29] A. P. Schnyder, S. Ryu, A. Furusaki, and A. W. Ludwig, in *AIP Conference Proceedings*, Vol. 1134 (AIP, 2009) pp. 10–21.
[30] E. Witten, Physics Letters B **117**, 324 (1982).
[31] E. Witten, Nuclear Physics, Section B **223**, 433 (1983).
[32] S. Elitzur and V. Nair, Nucl. Phys. **243**, 205 (1984).
[33] O. Bär and I. Campos, Nuclear Physics B-Proceedings Supplements **83**, 594 (2000).
[34] T. Fukui, T. Fujiwara, and Y. Hatsugai, Journal of the Physical Society of Japan **77**, 1 (2008), 0809.4532.
[35] T. Morimoto, H. C. Po, and A. Vishwanath, Physical Review B **95**, 1 (2017), 1703.02553.
[36] R. Kennedy and C. Guggenheim, Physical Review B **91**, 245148 (2015).
[37] L. S. Pontrjagin, in *Topological Library: Part 1: Cobordisms and Their Applications* (World Scientific, 2007) pp. 1–130.
[38] Please see Supplemental Material for additional details, which includes Ref. [46].
[39] X. Wan, A. M. Turner, A. Vishwanath, and S. Y. Savrasov, Phys. Rev. B **83**, 205101 (2011).
[40] This follows from Eq. (3), since $\mathcal{F}_{jk}$ and $\mathcal{A}_i$ are each third-order in $\hat{\mathbf{n}}$, making the Hopf invariant sixth-order, and thus even, in $\hat{\mathbf{n}}$. The former follow from $\mathcal{F}_{jk} = \frac{1}{8\pi}\hat{\mathbf{n}} \cdot (\partial_j \hat{\mathbf{n}} \times \partial_k \hat{\mathbf{n}})$ and $\partial_j \mathcal{A}_k - \partial_k \mathcal{A}_j = \mathcal{F}_{jk}$.
[41] S. A. Moses, J. P. Covey, M. T. Miecnikowski, D. S. Jin, and J. Ye, Nature Physics **13**, 13 (2017).
[42] L. De Marco, G. Valtolina, K. Matsuda, W. G. Tobias, J. P. Covey, and J. Ye, Science **363**, 853 (2019).
[43] J. P. Covey, L. De Marco, Ó. L. Acevedo, A. M. Rey, and J. Ye, New Journal of Physics **20**, 043031 (2018).
[44] L. Anderegg, L. W. Cheuk, Y. Bao, S. Burchesky, W. Ketterle, K.-K. Ni, and J. M. Doyle, arXiv preprint arXiv:1902.00497 (2019).
[45] Y. He and C.-C. Chien, Physical Review B **99**, 075120 (2019).
[46] R. Bott and R. Seeley, Comm. Math. Phys. **62**, 235 (1978).